

# Discovery of the optically bright, wide separation double quasar SDSS J1442+4055

A. V. Sergeev,<sup>1,2\*</sup> A. P. Zheleznyak,<sup>1,2</sup> V. N. Shalyapin,<sup>3,4</sup> and L. J. Goicoechea<sup>4</sup>

<sup>1</sup>*Institute of Radio Astronomy, Krasnoznamennaya 4, 61002 Kharkov, Ukraine*

<sup>2</sup>*Institute of Astronomy of Kharkov National University, Sumskaya 35, 61022 Kharkov, Ukraine*

<sup>3</sup>*Institute for Radiophysics and Electronics, National Academy of Sciences of Ukraine, 12 Proskura St., 61085 Kharkov, Ukraine*

<sup>4</sup>*Departamento de Física Moderna, Universidad de Cantabria, Avda. de Los Castros s/n, 39005 Santander, Spain*

Accepted XXX. Received YYY; in original form ZZZ

## ABSTRACT

Optically bright, wide separation double (gravitationally lensed) quasars can be easily monitored, leading to light curves of great importance in determining the Hubble constant and other cosmological parameters, as well as the structure of active nuclei and halos of galaxies. Searching for new double quasars in the SDSS-III database, we discovered SDSS J1442+4055. This consists of two bright images ( $r \sim 18\text{--}19$ ) of the same distant quasar at  $z = 2.575$ . The two quasar images are separated by  $\sim 2''.1$ , show significant parallel flux variations and can be monitored from late 2015. We also found other two double quasar candidates, SDSS J1617+3827 ( $z = 2.079$ ) and SDSS J1642+3200 ( $z = 2.264$ ), displaying evidence for the presence of a lensing object and parallel flux variations, but requiring further spectroscopic observations to be confirmed as lensed quasars.

**Key words:** gravitational lensing: strong – quasars: general – methods: data analysis – methods: observational

## 1 INTRODUCTION

Variability studies of gravitationally lensed quasars (GLQs) are a powerful means to study the Universe (e.g. Schneider, Kochanek & Wambsganss 2006). For example, time delays of GLQs are used to estimate cosmological parameters, primarily the current expansion rate of the Universe (the so-called Hubble constant; Oguri 2007; Suyu et al. 2010, 2013; Sereno & Paraficz 2014; Rathna Kumar, Stalin & Prabhu 2015). In addition, microlensing-induced flux variations reveal, among other things, the structure of quasars and properties of populations of stars (microlenses) in galaxies (e.g. Kochanek 2004; Eigenbrod et al. 2008; Poindexter, Morgan & Kochanek 2008; Dai et al. 2010; Morgan et al. 2010, 2012; Hainline et al. 2013; Mosquera et al. 2013; Blackburne et al. 2014; MacLeod et al. 2015). Multiwavelength intrinsic variability of GLQ images also produces valuable reverberation maps of emitting regions of quasars (Gil-Merino et al. 2012; Goicoechea et al. 2012), which will become in critical tools to check microlensing-derived source structures.

As searching for new lensed quasars and conducting subsequent monitoring campaigns are tasks of great relevance in cosmology, current quasar databases are being deeply mined to discover new GLQs (e.g. Oguri et al. 2006; Inada et al. 2012; Jackson et al. 2012; Elyiv et al. 2013; Buckley-Geer et al. 2014; Agnello et al. 2015a; Nord et al. 2015), and several techniques are being

developed to search for GLQs in ongoing and future surveys (e.g. Agnello et al. 2015b; Chan et al. 2015). The GLQ zoo includes rare phenomena consisting of two optically bright images ( $r < 20$ ) of the same distant quasar that are separated by  $\Delta\theta > 2''$ . Only five out of the 100 multiply-imaged systems in the CfA-Arizona Space Telescope Lens Survey (CASTLES) database<sup>1</sup> satisfy these conditions. Each of the optically bright, wide separation double quasars is of particular interest because it can be easily monitored with an 1–2m class telescope in average seeing conditions, and the time delay between its two images can be obtained from light curves and cross-correlation techniques (e.g. Poindexter et al. 2007; Shalyapin et al. 2008; Koptelova et al. 2012; Eulaers et al. 2013; Rathna Kumar et al. 2013). Detection of time delays between different optical bands (e.g. Koptelova et al. 2010) and uncorrelated (microlensing-induced) variations in light curves of the quasar images (e.g. Oscoz et al. 2013) is also possible.

The ongoing monitoring projects do not only focus on bright and widely-separated double quasars, although several targets belong to this type of systems. There are currently many cross-correlation techniques to determine time delays of GLQs (e.g. Liao et al. 2015), and the Cosmological Monitoring of Gravitational Lenses (COSMOGRAIL) is a collaboration targeting  $\sim 20$  GLQs to (mainly) measure their time delays (Tewes et al. 2012). The COSMOGRAIL website<sup>2</sup> incorporates a list of main publications,

<sup>1</sup> <https://www.cfa.harvard.edu/castles/>

<sup>2</sup> <http://cosmograil.epfl.ch>

\* E-mail: alexey.v.sergeev@gmail.com

light curves and other relevant information. This large collaboration uses 1–2m telescopes in both hemispheres, and has published light curves and time delays of 7 GLQs with optically bright images. Two of them are widely-separated doubles (Eulaers et al. 2013; Rathna Kumar et al. 2013), three are quads with some widely-separated images, and two are doubles with  $\Delta\theta \sim 1''$ . Other groups are also involved in similar programmes. For example, the Gravitational Lenses and Dark Matter (GLENDAMA) project is conducting an optical monitoring of  $\sim 10$  bright GLQs with different angular sizes<sup>3</sup>. The GLENDAMA team uses a 2m robotic telescope in the north hemisphere with the purpose of measuring time delays, and analysing intrinsic and extrinsic (microlensing) flux variations (e.g. Goicoechea, Shalyapin & Ullán 2010).

In this paper, we present our ongoing search for GLQs in the Sloan Digital Sky Survey III (SDSS-III) database (Eisenstein et al. 2011). The selection of GLQ candidates and the corresponding identification campaigns are described in Sec. 2. All candidates are composed of two point-like sources: one of them is a confirmed quasar and the other belongs to an unknown class. Our spectroscopic observations confirm the GLQ nature of SDSS J1442+4055, which has been independently discovered by More et al. (2015). In Sec. 3, using new deep imaging in the  $r$  band, we present astrophotometric solutions and lens models for this optically bright, wide separation lens system. Our conclusions and future prospects appear in Sec. 4.

## 2 SELECTION AND IDENTIFICATION OF GLQ CANDIDATES

### 2.1 Samples

Our first sample (S1) of GLQ candidates is based on the SDSS-III Data Release 9 (Ahn et al. 2012). We used the Data Release 9 Quasar (DR9Q) catalog containing 87 822 spectroscopically confirmed objects (Paris et al. 2012), as well as *gri* frames including these quasars and other surrounding sources. We initially checked for the presence of some point-like source in the vicinity ( $1\text{--}6''$  apart) of each DR9Q quasar over the redshift interval  $0.8 < z < 4$  and brighter than  $r = 21$ . After finding an association, the similarity of colours of the quasar and its companion was probed. Specifically, we estimated the average magnitude difference  $\text{AMD} = (\Delta g + \Delta r + \Delta i)/3$  for each pair, and then selected pairs satisfying the constraints  $d_g < 0.4$ ,  $d_r < 0.4$  and  $d_i < 0.4$ , where  $d_g = \Delta g - \text{AMD}$ ,  $d_r = \Delta r - \text{AMD}$  and  $d_i = \Delta i - \text{AMD}$ . After visual inspection of the selected targets, we obtained a sample of 39 candidates.

To construct a second sample (S2), we used the SDSS-III DR10 (Ahn et al. 2014; Paris et al. 2014) and adopted a selection method different from the previous one (see above). We concentrated on quasars in the range  $\text{RA} = 180\text{--}360^\circ$ , over the redshift interval  $1 < z < 5$  and brighter than  $r = 20$ . We then searched for neighbour point-like sources at  $\Delta\theta \leq 6''$ . For the widely-separated quasar-companion pairs ( $\Delta\theta > 2''$ ), a detailed colour test was also done. Using the corresponding *ugriz* frames, we compared colours of quasars and their companions, and selected pairs satisfying the constraints  $|\Delta(u - g)| < 0.4$ ,  $|\Delta(g - r)| < 0.2$ ,  $|\Delta(r - i)| < 0.2$  and  $|\Delta(i - z)| < 0.4$ . After visual inspection, we selected 17

GLQ candidates for the S2 sample<sup>4</sup>. None of these new targets is included in S1.

Our selection criteria differ from those used to make the statistical lens sample of the SDSS Quasar Lens Search (SQLS; Oguri et al. 2006; Inada et al. 2012), since we focus on double quasar candidates with separations of a few arcseconds, which are within a larger cosmic volume and cover a wider range of magnitudes. However, the SQLS database<sup>5</sup> also contains additional double quasars that are not included in the statistical sample (e.g. Inada et al. 2009).

### 2.2 Follow-up observations of selected subsamples

From the whole S1 sample in Sec. 2.1, we took a subsample (SS1) of three targets to perform follow-up observations (see Table 1). We focused on  $\sim 10\%$  of the initial sample in the RA interval  $110\text{--}120^\circ$ . These three SS1 candidates in Table 1 have a large separation, and the immediate goal of the observations was to check the efficiency of our first selection method and try to discover some new GLQ. We attempted to obtain decent spectra for all SS1 targets in 2014. However, the spectra of the faintest candidate were very noisy, so it was also imaged. For this candidate, in Sec. 2.3, we only present the analysis of its astro-photometric data.

We selected  $\sim 80\%$  of the S2 sample, i.e., 14 out of the 17 initial candidates (see Table 1), to make a second subsample in the RA interval  $180\text{--}330^\circ$  (SS2). We first obtained follow-up images for 13 SS2 candidates at the Maidanak Astronomical Observatory (MAO) in 2015 June, and then attempted to conduct spectroscopic observations of each target whose follow-up images showed evidence for both a lensing galaxy and a variable companion. As almost all (12) SS2-MAO targets have a quasar at  $z > 2$ , the presence of a residual object (residual signal above the noise level) was considered as evidence for a lensing galaxy (see Sec. 2.3). In addition, companion sources with flux variations (absolute differences between their SDSS and MAO magnitudes in the  $r$  band) of  $\geq 0.1$  mag were identified as variable objects. Unfortunately, we could not complete the spectroscopic observations due to observing constraints. However, we obtained spectra for the only SS2 target that was not imaged during the intensive observational campaign in 2015 June. This last candidate had weaker observing constraints than the pending targets showing flux variations and residual sources.

### 2.3 Results

SDSS J0734+2733 is the brightest candidate, i.e., two components with  $r \sim 17$ . This was observed with the integral field spectrograph (FRODOSpec) on the 2m Liverpool Telescope (LT). A 3200 s exposure on a dark night under normal seeing conditions was taken with this instrument. FRODOSpec is characterised by a field of view and a spatial scale of  $\sim 10'' \times 10''$  and  $0''.8 \text{ pixel}^{-1}$ , respectively, and allows us to extract individual spectra for two point-like sources separated by a few pixels (Shalyapin & Goicoechea 2014). We also note that the spectrograph has two independent arms, allowing simultaneous spectroscopy at blue and red wavelengths. However, the sensitivity of its red arm is significantly higher, so we only show

<sup>4</sup> To achieve a reasonable balance between compact ( $\Delta\theta \sim 1\text{--}2''$ ) and wide separation candidates, we did not consider targets with  $\Delta\theta > 2''$  in the RA interval  $180\text{--}210^\circ$

<sup>5</sup> <http://www-utap.phys.s.u-tokyo.ac.jp/~sdss/sqls/lens.html>

<sup>3</sup> [http://grupos.unican.es/glendama/LQLM\\_results.htm](http://grupos.unican.es/glendama/LQLM_results.htm)

**Table 1.** Identification of GLQ candidates. For both subsamples (SS1 and SS2), besides the name, redshift and position (J2000) of the quasars, it is also shown the separation between each quasar and its previously unidentified companion, as well as the follow-up observations. The last column informs about our main results using deep imaging and/or spectroscopy.

Quasar	$z$	RA (°)	DEC. (°)	$\Delta\theta$ (")	Follow-up observations		GLQ
					Imaging (Date)	Spectroscopy (Date)	
SS1							
SDSS J0734+2733	1.918	113.52813	+27.56545	2.55		LT/FRODOSpec (2014 Dec 20)	No
SDSS J0735+2036	2.189	113.89411	+20.60950	3.68		TNG/DOLORES (2014 Mar 02)	No
SDSS J0755+1400	0.845	118.83309	+14.01166	2.14	NOT/ALFOSC (2014 Mar 21)		Unlikely
SS2							
SDSS J1239+4447	2.037	189.76377	+44.78371	1.77	AZT-22/SNUCam (2015 Jun 05)		Unlikely
SDSS J1410+2340	2.449	212.51833	+23.68192	3.58	AZT-22/SNUCam (2015 Jun 07)		Unlikely
SDSS J1442+4055	2.575	220.72826	+40.92655	2.07	AZT-22/SNUCam (2015 Jun 10)	LT/SPRAT (2015 Aug 29)	Yes
SDSS J1523+1220	2.403	230.81149	+12.33632	2.19	AZT-22/SNUCam (2015 Jun 17)		Unlikely
SDSS J1526+0151	3.167	231.63047	+01.85088	1.41	AZT-22/SNUCam (2015 Jun 11)		Unlikely
SDSS J1554+2616	2.321	238.54804	+26.27660	2.16	AZT-22/SNUCam (2015 Jun 18)		Unlikely*
SDSS J1600+1028	1.535	240.06076	+10.48122	1.28	AZT-22/SNUCam (2015 Jun 16)		Unlikely
SDSS J1617+3827	2.079	244.47052	+38.46030	2.12	AZT-22/SNUCam (2015 Jun 15)		Yes?
SDSS J1619+1621	2.426	244.87857	+16.35632	2.63	AZT-22/SNUCam (2015 Jun 18)		Unlikely
SDSS J1642+3200	2.263	250.71282	+32.00811	2.91	AZT-22/SNUCam (2015 Jun 11)		Yes?
SDSS J1648+3400	2.144	252.24318	+34.01664	1.37	AZT-22/SNUCam (2015 Jun 07)		Unlikely
SDSS J1655+1948	3.261	253.93153	+19.81310	3.85		LT/SPRAT (2015 September 10)	No
SDSS J2053-0100	2.207	313.38756	-01.01622	1.43	AZT-22/SNUCam (2015 Jun 17)		Unlikely
SDSS J2153+2732	2.216	328.31784	+27.54302	3.62	AZT-22/SNUCam (2015 Jun 20)		Unlikely

\* Identified as a quasar+star system by [More et al. \(2015\)](#).

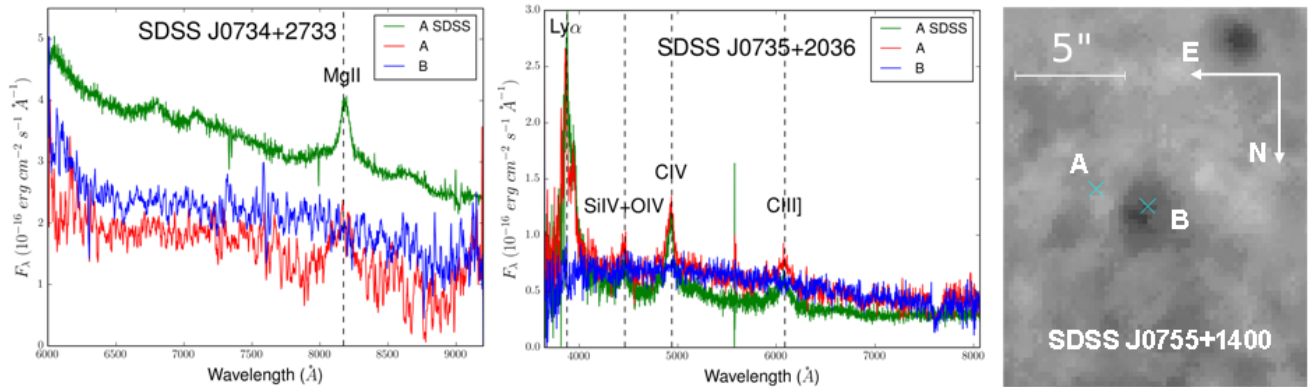


**Figure 1.** Follow-up observations of SS1 candidates. Left and middle: spectra of the two components (A and B) of SDSS J0734+2733 and SDSS J0735+2036. In each panel, we also show the SDSS spectrum of the quasar (A) for comparison purposes. Right:  $I$ -band residual frame of SDSS J0755+1400. This is an inverted greyscale image, so brighter sources correspond to darker zones. Here, B is the confirmed quasar and A its companion.

the red spectra of SDSS J0734+2733 in the left panel of Fig. 1. The original FRODOSpec/red-arm data (spectral resolving power  $R \sim 2200$ ) have been smoothed using a rectangular smoothing window of  $24 \text{ \AA}$ . While the confirmed quasar (component A; red line) shows a Mg II emission line near  $8200 \text{ \AA}$ , this feature is absent in the spectrum of its companion (component B; blue line). Hence, we conclude that SDSS J0734+2733 is not a double quasar.

SDSS J0735+2036 was observed with the Device Optimized for the Low Resolution (DOLORES) on the 3.6m Telescopio Nazionale Galileo (TNG). We used the LR-B grism ( $R \sim 600$  and  $0''.25 \text{ pixel}^{-1}$ ) and the  $1''.5$  long slit, putting this slit in the direction

joining both optically bright components ( $r \sim 19$ ). The spectroscopic exposure of 1200 s was done on a dark night. In the middle panel of Fig. 1, we depict the TNG/DOLORES spectra of the quasar (component A; red line) and the previously unidentified object (component B; blue line). The continuum of B is similar to that of the quasar, but there are no emission lines superimposed. Thus, the companion object is likely a star.

Regarding SDSS J0755+1400 ( $r \sim 19-20$ ), we obtained  $I$ -band exposures with the Andalucia Faint Object Spectrograph and Camera (ALFOSC) on the 2.5m Nordic Optical Telescope (NOT). This camera has a spatial scale of  $0''.19 \text{ pixel}^{-1}$ , which makes it

a suitable instrument, in good seeing conditions, to try to detect a possible lensing galaxy between the two sources. Unfortunately, only half of individual frames were useful, and these were combined to produce a single deep exposure (1800 s of dark time under good seeing conditions). We then subtracted two point-spread functions (PSFs) from the NOT/ALFOSC combined frame of the candidate, using nearby stars as PSF templates. In the right panel of Fig. 1, we display the residual frame after subtracting the two point-like sources centred at the green crosses. Actually the residual signal was smoothed with a median filter in circular neighborhoods (4-pixel radius), and contains a possible very faint source ( $I > 22$ ) close to the quasar B. However, this source (if real) is not expected to be the lensing galaxy of a quasar at  $z = 0.845$  because so faint lensing objects are usually associated with GLQs at  $z > 3$  (see the CASTLES database<sup>1</sup>). Assuming an early-type lens galaxy, we can also infer the expected value of the lens magnitude in the  $I$  band as a function of the lens redshift  $z_{\text{lens}}$  (e.g. Rusin et al. 2003). The NOT/ALFOSC data are against the GLQ nature of SDSS J0755+1400, since the lens galaxy should have  $I < 19$  at  $z_{\text{lens}} \leq 0.8$ .

Using the Seoul National University Camera (SNUCam) on the 1.5m AZT-22 Telescope ( $0''.27 \text{ pixel}^{-1}$ ) at the MAO, we obtained 3600 s ( $6 \times 600$  s) exposures in the SDSS  $r$  and/or  $i$  bands for 13 out of the 14 SS2 candidates (see Table 1). Most individual frames were taken under good seeing conditions ( $\text{FWHM} \leq 1''$ ), and only three combined  $r$ -band frames led to residual signals above the noise level, i.e., residual sources with  $r \leq 23$ . These combined frames are shown in the left panels of Fig. 2. After subtracting two PSFs within the regions containing quasar-companion (A-B) pairs, the residual frames are also presented in the right panels of Fig. 2. We only focused on the three targets having an associated residual source (R), which was interpreted as evidence of the existence of a lensing galaxy. The average redshift and separation for the 13 candidates are  $\langle z \rangle = 2.3$  and  $\langle \Delta\theta \rangle = 2''.2$ , so there is a weak constraint  $r \leq 23$  on  $r$ -band magnitudes of possible early-type lens galaxies at  $z_{\text{lens}} \leq 2$ . We also checked the variability of the companion sources (comparing their new MAO magnitudes with the corresponding SDSS data), since quasars are variable objects. This kind of test has been proposed by Kochanek et al. (2006) and Buckley-Geer et al. (2014) among others. The 3 companions are variable sources because we detected appreciable changes in their  $r$ -band magnitudes, i.e.,  $|r_{\text{SDSS}} - r_{\text{MAO}}| \geq 0.1$ .

SDSS J1442+4055 has two bright components ( $r \sim 18-19$ ), and the residual object appears in the expected position for a main lensing galaxy. A possible secondary lens also lies southwest of this object in the top right panel of Fig. 2. Through PSF photometry in the  $r$  band (using standard IRAF<sup>6</sup> tasks), we calculated magnitude differences between two epochs separated by  $\sim 10$  years: SDSS(2003 March) – MAO(2015 June). For field stars, these differences were only about  $\pm 0.01$ , while we obtained highly significant flux decrements of  $\sim 0.1-0.2$  magnitudes for both components. These are strong arguments in favour of the GLQ nature of SDSS J1442+4055, and thus, we selected this target for spectroscopic follow-up observations with the highest priority. The other two candidates: SDSS J1617+3827 ( $r \sim 19-21$ ) and SDSS J1642+3200 ( $r \sim 18-21$ ), do not show significant residues on the

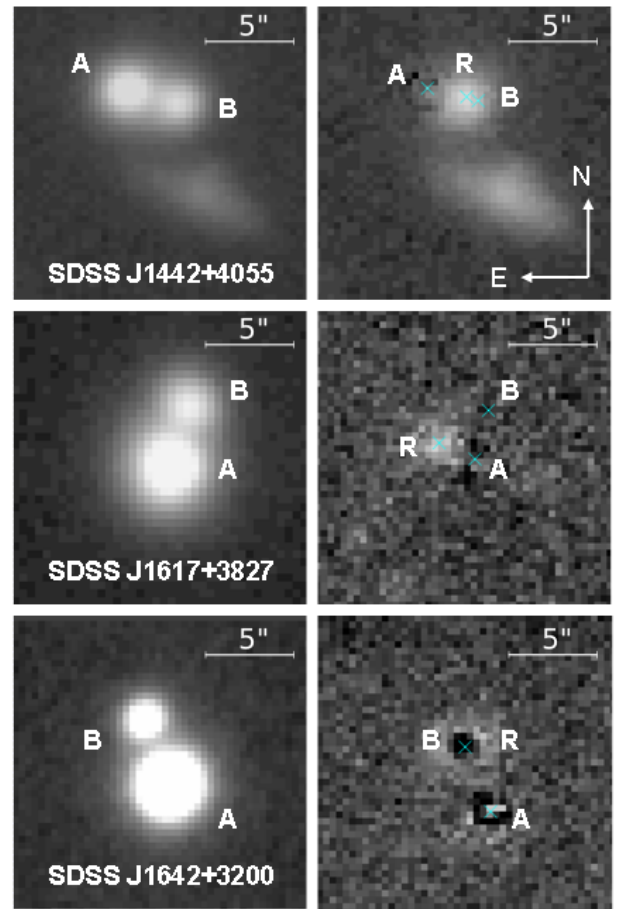


**Figure 2.** MAO  $r$ -band observations of three SS2 candidates. Left: combined 3600-s exposures of the quasar-companion (A-B) pairs. Right: residual frames. Each frame includes one residual object (R).

lines joining their components (see the middle and bottom right panels of Fig. 2). The residual objects are located northeast of the bright quasar with  $r \sim 19$  (SDSS J1617+3827) or around the faint companion object with  $r > 20$  (SDSS J1642+3200). Additionally, the quasars and their companions have experienced flux decrements that exceed the noise level (0.01 mag) in factors from 3 to 30. Therefore, these two candidates also deserve more attention, and they were selected as secondary targets for spectroscopy. Unfortunately, we were not able to get decent spectra for both targets.

We observed SDSS J1442+4055 with the Spectrograph for the Rapid Acquisition of Transients (SPRAT) on the 2m LT. Although the sky was relatively bright, the strong evidence for a GLQ and the near end of the target visibility window justified urgent spectroscopic observations. Using the blue grating and the  $1''.8$  long slit ( $R \sim 350$  and  $0''.44 \text{ pixel}^{-1}$ ), we took five 600 s exposures in normal seeing conditions ( $\text{FWHM} \sim 1''.3$ ). The top panel of Fig. 3 shows the combined (3000 s) spectra of A (quasar) and B (companion source), which incorporate Ly $\alpha$ +N V, Si IV+O IV], C IV and C III] emission lines at very similar wave-

<sup>6</sup> IRAF is distributed by the National Optical Astronomy Observatories, which are operated by the Association of Universities for Research in Astronomy, Inc., under cooperative agreement with the National Science Foundation

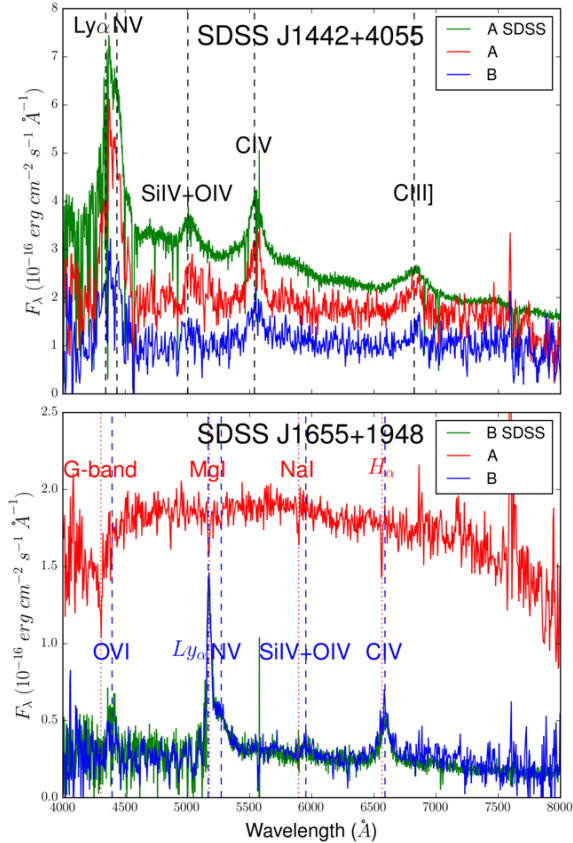


**Figure 3.** LT/SPRAT spectroscopic observations of two SS2 targets. Top: spectra of the two components (A and B) of SDSS J1442+4055. The SDSS spectrum of the quasar (A) is also displayed in this panel. Bottom: spectra of the two components (A and B) of SDSS J1655+1948. We also show the SDSS spectrum of the quasar (B).

lengths. A cross-correlation between the two spectra proved that their redshifts are identical<sup>7</sup>, and this corroborated the GLQ nature of SDSS J1442+4055.

We also obtained SPRAT spectra for the only SS2 target that was not observed at the MAO. The candidate SDSS J1655+1948 consists of a relatively faint quasar (B) with  $r \sim 20$  and a bright companion (A) with  $r \sim 18$ , and its 3000 s spectra are depicted in the bottom panel of Fig. 3. For this GLQ candidate, the A component is a star whose spectrum incorporates several absorption lines at  $z \sim 0$ . We failed again in a positive identification of a candidate selected by standard methods (see Sec. 2.1), and this stresses the efficiency in detecting GLQs using more sophisticated selection criteria, i.e., existence of a residual object and variable components.

### 3 SDSS J1442+4055

The MAO  $r$ -band imaging of SDSS J1442+4055 (FWHM  $\sim 1''$ ) was also used to infer astro-photometric solutions for the new lens system. Through the GALFIT software (Peng et al. 2002), this was

<sup>7</sup> More properly, the redshift difference is  $\Delta z < 0.001$ , where  $\Delta z = 0.001$  corresponds to a pixel along the dispersion axis

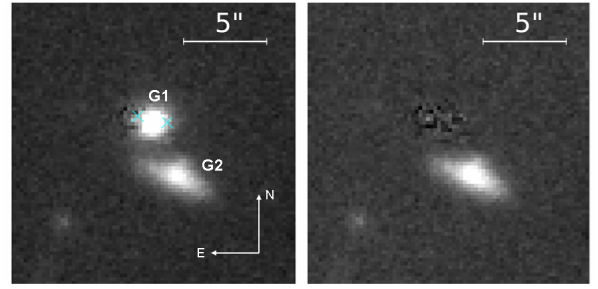


**Figure 4.** GALFIT model of SDSS J1442+4055 in the  $r$  band. This model includes three ingredients: two PSFs (quasar images) and the convolution of a 2D Sérsic profile with the PSF (main lensing galaxy G1). We show the residual signal after subtracting only the quasar images (left panel) and after subtracting the global solution (right panel).

modelled as two PSFs (quasar images) plus a standard galaxy profile convolved with the PSF. We considered a 2D Sérsic profile (Sérsic 1963) for the main lensing galaxy, since it can describe light distributions for different types of galaxies. In the left and right panels of Fig. 4, we display the residual signal after subtracting the two quasar images and the final residues after subtracting the global best fit (quasar images + main lensing galaxy), respectively. The main lens (G1) and the secondary lens (G2) are clearly resolved in the left panel of Fig. 4. Apart from the solution leaving the concentration index ( $n$ ) as a free parameter (Sérsic profile), we also used a de Vaucouleurs profile for G1 to obtain a second solution, i.e., fixing  $n = 4$ , rather than leaving it as a free parameter (see Table 2). This is a reasonable profile for early-type galaxies and galactic bulges, and it may be useful for extracting quasar fluxes from optical frames in monitoring campaigns (e.g. Shalyapin et al. 2008). However, the reduced chi-squared value is 1.8, so the  $1\sigma$  confidence intervals that we give in Table 2 should be taken with caution.

SDSS J1442+4055 has been independently discovered by More et al. (2015). When we were writing this report, More et al. (2015) announced the discovery of thirteen GLQs, including SDSS J1442+4055 between their confirmed lens systems. They used a 900 s  $i$ -band exposure with the 2.4m Hiltner Telescope to model the system, whereas our fits were based on an  $r$ -band combined frame with an equivalent exposure time (2.4m telescope) of 1400 s. We note that our estimation of  $r_{G1}$  in Table 2 coincides with the  $(g_{G1} + i_{G1})/2$  value from Table 3 of More et al. Although there is also agreement in the values of  $e$  and  $r_{\text{eff}}$  (the Sérsic profile led to  $r_{\text{eff}} \sim 1''$  and a large index  $n > 4$ ), our  $\theta_e$  values are separated by  $\sim 90^\circ$  from the More et al.'s solution for the position angle.

Even though the redshift of the main lensing galaxy (G1) is still unknown, the current SDSS-MAO data give a hint as to the  $z_{\text{lens}}$  value. The SDSS spectrum of the A image shows the existence of an absorption system at  $z_{\text{abs}} = 1.946$ , which was identified from 12 different absorption features in the wavelength range 4500–8500 Å. However, the Rusin et al.'s scheme (Rusin et al. 2003) is in clear disagreement with a bright lens ( $r \sim 19.5$ ; see Table 2) at  $z_{\text{lens}} \sim 2$ , so the distant absorption system is most likely not linked to G1. We may also consider a second scenario where G1 is physically associated with G2 ( $r \sim 20$ ). As the SDSS database includes a photometric redshift for G2 ( $0.32 \pm 0.05$ ),  $z_{\text{lens}}$  would be  $\sim 0.3$ – $0.4$ . This lens redshift is in good agreement with the MAO brightness of G1, and thus, the gravitational lens could consist of two galaxies at similar moderate values of  $z$ .

**Table 2.** Astro-photometric solution for SDSS J1442+4055 in the  $r$  band. Here,  $(x_B, y_B)$  is the position of B, and the last six parameters correspond to G1 (de Vaucouleurs profile): position  $(x_{G1}, y_{G1})$ , magnitude  $(r_{G1})$ , effective radius  $r_{\text{eff}}$ , ellipticity  $e$ , and position angle of the major axis  $\theta_e$  (it is measured east of north).

$x_B$ (")	$y_B$ (")	$x_{G1}$ (")	$y_{G1}$ (")	$r_{G1}$ (mag)	$r_{\text{eff}}$ (")	$e$	$\theta_e$ ( $^\circ$ )
$2.096 \pm 0.003$	$-0.506 \pm 0.001$	$1.342 \pm 0.013$	$-0.344 \pm 0.008$	$19.47 \pm 0.01$	$0.59 \pm 0.02$	$0.19 \pm 0.04$	$-12 \pm 6$

We also modelled SDSS J1442+4055 using the relative astrometry in Table 2 and the  $i$ -band flux ratio by More et al. (2015), as well as a singular isothermal sphere (SIS) mass model in a standard cosmology (e.g. Schneider, Kochanek & Wambsganss 2006). The LENSMODEL software (Keeton 2001) led to a solution with  $\chi^2 \gg 1$ , indicating we need to improve our model. The simplest option is to add ellipticity to the SIS mass distribution of G1. Thus, we used the LENSMODEL package to find the singular isothermal ellipsoid (SIE) solution for the astro-photometric constraints. The number of model parameters was the same as the number of observational constraints, and the new solution was characterized by a mass scale  $b \sim 1''.08$ , an ellipticity  $e \sim 0.017$ , a mass orientation of about  $-60^\circ$  and  $\chi^2 \sim 0$ . Although the ellipticity and orientation of the mass do not coincide with the ellipticity and orientation for the light distribution of G1 (see the two last columns in Table 2), we remark that we are dealing with an effective mass distribution, since the secondary lens (G2) was not modelled in any way. For this effective lens model (SIE), the expected time delay is  $\sim 40$  days if  $z_{\text{lens}} = 0.4$  (A is leading).

#### 4 CONCLUSIONS AND FUTURE WORK

Using the SDSS-III DR9 (Ahn et al. 2012; Paris et al. 2012) and DR10 (Ahn et al. 2014; Paris et al. 2014), we have searched for new double quasars with separations of  $1-6''$ . As expected, samples of a few candidates selected from standard criteria (i.e., a quasar and a point-like companion source, having both similar colours) were largely inefficient tools to find new GLQs (e.g. Inada et al. 2012). For this reason, we introduced two additional ingredients in the selection procedure: presence of a residual source (lensing galaxy?) in a new deep exposure, and detection of flux variations by comparing the SDSS imaging and the new non-SDSS exposure.

After an observational campaign at the Maidanak Astronomical Observatory, we found three GLQ candidates satisfying all our selection criteria. The most promising target (SDSS J1442+4055) was spectroscopically observed in 2015 August, showing two identical spectra for the quasar and its companion (see also More et al. 2015). This is an optically bright, wide separation double quasar whose images appreciably vary in parallel on a 10-year timescale (see Sec. 2.3). Therefore, SDSS J1442+4055 is an excellent target to be monitored with an 1–2m class telescope from late 2015. Besides light curves of the two quasar images, new spectroscopy and deep imaging are required to accurately determine the lens redshift  $z_{\text{lens}}$  and the astro-photometric parameters. The current astro-photometric data suggest that  $z_{\text{lens}} \sim 0.3-0.4$ , where the main lens would be the galaxy G1, while another neighbor galaxy (G2) would also contribute to the gravitational mirage. Spectroscopic observations of the other two GLQ candidates (SDSS J1617+3827 and SDSS J1642+3200) are also needed to determine their GLQ nature.

The new lens system SDSS J1442+4055 is now included in the GLENDAMA list of GLQs, so it will be observed with the LT, the 10.4m Gran Telescopio Canarias and other facilities. We also plan to perform a spectroscopic follow-up of the two variable targets

with residual sources (SDSS J1617+3827 and SDSS J1642+3200), as well as two additional variable targets that do not show residual sources with  $r \leq 23$  (SDSS J2053-0100 and SDSS J2153+2732; see Table 1). In the near future, we will also explore the feasibility to find new GLQs in the SDSS-III and other databases, by using pairs of unidentified point-like sources showing evidence for variability (e.g. Kochanek et al. 2006; Buckley-Geer et al. 2014).

#### ACKNOWLEDGEMENTS

We wish to thank the anonymous referee and Anupreeta More for useful suggestions and comments that have helped to improve the original manuscript. The observations at the Maidanak Astronomical Observatory were supported by the ISON project. We thank Seoul National University for equipping the AZT-22 Telescope with a modern CCD camera. This report is also based on observations made with the Liverpool Telescope (Prog. XCL04BL2), the Nordic Optical Telescope (Prog. SST2014-057) and the Telescopio Nazionale Galileo (Prog. A28DDT8), operated on the island of La Palma by the Liverpool John Moores University (with financial support from the UK Science and Technology Facilities Council), the Nordic Optical Telescope Scientific Association and the Fundación Galileo Galilei of the INAF (Istituto Nazionale di Astrofisica), respectively, in the Spanish Observatorio del Roque de los Muchachos of the Instituto de Astrofísica de Canarias. We thank the staff of all used telescopes for a kind interaction before, during and after the observations. We also used data taken from the SDSS-III web site (<http://www.sdss3.org/>), and we are grateful to the SDSS-III collaboration for doing that public database. This research has been supported by the Spanish Department of Research, Development and Innovation grant AYA2013-47744-C3-2-P (GLENDAMA project), and the University of Cantabria.

#### REFERENCES

- Agnello A. et al., 2015a, MNRAS, 454, 1260  
Agnello A., Kelly B. C., Treu T., Marshall P. J., 2015b, MNRAS, 448, 1446  
Ahn C. P. et al., 2012, ApJS, 203, 21  
Ahn C. P. et al., 2014, ApJS, 211, 17  
Blackburne J. A., Kochanek C. S., Chen B., Dai X., Chartas G., 2014, ApJ, 789, 125  
Buckley-Geer E.J., Dark Energy Survey Collaboration, 2014, AAS Meeting 223, No. 248.01  
Chan J. H. H., Suyu S. H., Chiueh T., More A., Marshall P. J., Coupon J., Oguri M., Price P., 2015, ApJ, 807, 138  
Dai X., Kochanek C. S., Chartas G., Kozlowski S., Morgan C. W., Garmire G., Agol E., 2010, ApJ, 709, 278  
Eigenbrod A., Courbin F., Meylan G., Agol E., Anguita T., Schmidt R. W., Wambsganss J., 2008, A&A, 490, 933  
Eisenstein D. J. et al., 2011, AJ, 142, 72  
Elyiv A., Melnyk O., Finet F., Pospieszalska-Surdej A., Chiappetti L., Pierre M., Sadibekova T., Surdej J., 2013, MNRAS, 434, 3305  
Eulaers E. et al., 2013, A&A, 553, 121  
Gil-Merino R., Goicoechea L. J., Shalyapin V. N., Braga V. F., 2012, ApJ, 744, 47

- Goicoechea L. J., Shalyapin V. N., Ullán A., 2010, *Advances in Astronomy*, 2010, 347935
- Goicoechea L. J., Shalyapin V. N., Gil-Merino R., Braga V. F., 2012, *Journal of Physics Conference Series*, 372, 012058
- Hainline L. J. et al., 2013, *ApJ*, 774, 69
- Inada N. et al., 2009, *AJ*, 137, 4118
- Inada N. et al., 2012, *AJ*, 143, 119
- Jackson N., Rampadarath H., Ofek E. O., Oguri M., Shin M.-S., 2012, *MNRAS*, 419, 2014
- Keeton C. R., 2001, arXiv:astro-ph/0102340
- Kochanek C. S., 2004, *ApJ*, 605, 58
- Kochanek C. S., Mochejska1 B., Morgan N. D., Stanek K. Z., 2006, *ApJ*, 637, L73
- Koptelova E., Oknyanskij V. L., Artamonov B. P., Burkhonov O., 2010, *MNRAS*, 401, 2805
- Koptelova E. et al., 2012, *A&A*, 544, 51
- Liao K. et al., 2015, *ApJ*, 800, 11
- MacLeod C. L. et al., 2015, *ApJ*, 806, 258
- More A. et al., 2015, preprint (arXiv:1509.07917)
- Morgan C. W., Kochanek C. S., Morgan N. D., Falco E. E., 2010, *ApJ*, 712, 1129
- Morgan C. W. et al., 2012, *ApJ*, 756, 52
- Mosquera A. M., Kochanek C. S., Chen B., Dai X., Blackburne J. A., Charatas G., 2013, *ApJ*, 769, 53
- Nord B. et al., 2015, AAS Meeting 225, No. 255.21
- Oguri M., 2007, *ApJ*, 660, 1
- Oguri M. et al., 2006, *AJ*, 132, 999
- Oscos A., Serra-Ricart M., Mediavilla E., Muñoz J. A., 2013, *ApJ*, 779, 144
- Pâris I. et al., 2012, *A&A*, 548, 66
- Pâris I. et al., 2014, *A&A*, 563, 54
- Peng C. Y., Ho L. C., Impey C. D., Rix H.-W., 2002, *AJ*, 124, 266
- Poindexter S., Morgan N., Kochanek C. S., Falco, E. E., 2007, *ApJ*, 660, 146
- Poindexter S., Morgan N., Kochanek C. S., 2008, *ApJ*, 673, 34
- Rathna Kumar S., Stalin C. S., Prabhu T. P., 2015, *A&A*, 580, 38
- Rathna Kumar S. et al., 2013, *A&A*, 557, 44
- Rusin D. et al., 2003, *ApJ*, 587, 143
- Schneider P., Kochanek C. S., Wambsganss, J., 2006, in Meylan G., Jetzer P., North P., eds, Proc. 33rd Saas-Fee Advanced Course, Gravitational Lensing: Strong, Weak & Micro. Springer, Berlin
- Sereno M., Paraficz D., 2014, *MNRAS*, 437, 600
- Sérsic J. L., 1963, *Boletín de la Asociación Argentina de Astronomía*, 6, 41
- Shalyapin V. N., Goicoechea L. J., 2014, *AN*, 335, 428
- Shalyapin V. N., Goicoechea L. J., Koptelova E., Ullán A., Gil-Merino R., 2008, *A&A*, 492, 401
- Suyu S. H., Marshall P. J., Auger M. W., Hilbert S., Blandford R. D., Koopmans L. V. E., Fassnacht C. D., Treu T., 2010, *ApJ*, 711, 201
- Suyu S. H. et al., 2013, *ApJ*, 766, 70
- Tewes M. et al., 2012, *The Messenger*, 150, 49

This paper has been typeset from a  $\text{\TeX}/\text{\LaTeX}$  file prepared by the author.